Carbon dioxide uptake of a forested region in southwest France derived from airborne CO_2 and CO measurements in a quasi-Lagrangian experiment

Sandra Schmitgen,[1,2] Heiner Geiß,[3] Philippe Ciais,[1] Bruno Neininger,[4] Yves Brunet,[5] Markus Reichstein,[6,7] Dieter Kley,[3] and Andreas Volz-Thomas[3]

Received 7 November 2003; revised 8 March 2004; accepted 16 March 2004; published 29 July 2004.

[1] This paper presents a Lagrangian budgeting approach to quantify the uptake of CO_2 by vegetation at horizontal scales of several tens of kilometers. For this purpose, CO_2 and meteorological parameters were measured from a small aircraft during four flights in June 2001 over a flat homogeneous and productive temperate forest in the Landes region (southwestern France). Additional CO measurements were made in order to identify and quantify the potential influence of anthropogenic emissions on the net CO_2 flux derived from the measurements. For one of four flights, Lagrangian conditions were nearly perfectly fulfilled. On average, the CO_2 mixing ratio in the boundary layer decreased at a rate of 0.11 ppm km^{-1}, yielding an average CO_2 uptake by the forest of 16 ± 2.5 μmol m^{-2} s^{-1} between 1230 and 1430 UT. Our result is about 15% smaller than the local net ecosystem exchange measured by eddy covariance at a tower north of the flight domain and about 12% higher than a regional estimate based on remote sensing data for the whole experimental area. The contribution of anthropogenic emissions to the regional CO_2 budget was estimated from the CO measurements to be to <0.5 μmol m^{-2} s^{-1}. *INDEX TERMS:* 0315 Atmospheric Composition and Structure: Biosphere/atmosphere interactions; 0322 Atmospheric Composition and Structure: Constituent sources and sinks; 0394 Atmospheric Composition and Structure: Instruments and techniques; 1615 Global Change: Biogeochemical processes (4805); 3307 Meteorology and Atmospheric Dynamics: Boundary layer processes; *KEYWORDS:* carbon dioxide flux, regional CO_2 budget, carbon monoxide

Citation: Schmitgen, S., H. Geiß, P. Ciais, B. Neininger, Y. Brunet, M. Reichstein, D. Kley, and A. Volz-Thomas (2004), Carbon dioxide uptake of a forested region in southwest France derived from airborne CO_2 and CO measurements in a quasi-Lagrangian experiment, *J. Geophys. Res.*, *109*, D14302, doi:10.1029/2003JD004335.

1. Introduction

[2] The Kyoto protocol, whilst calling for significant reductions in the emissions of CO_2 and other greenhouse gases, also allows the countries to account for biological sinks, i.e., fixation of carbon by terrestrial ecosystems. Because of the important political consequences, there is a strong need for an independent verification of the reported emissions and particularly the sinks, which must be firmly linked to field observations.

[3] The global atmospheric carbon budget is rather well constrained by the atmospheric trends of CO_2 concentrations and O_2/N_2 ratios as monitored at remote oceanic stations [*Intergovernmental Panel on Climate Change* (*IPCC*), 2001]. Likewise, eddy covariance flux measurements provide reasonably accurate measurements of local ecosystem carbon balances on spatial scales of a few hundreds of meters [*Baldocchi et al.*, 1996; *Valentini et al.*, 2000; *Wofsy et al.*, 1993]. However, very little experimental information exists on the carbon budget at regional scales, ranging from a few hundred to several thousands of square kilometers for individual ecosystems to political units and continents. These budgets are estimated either by downscaling from the global scale or by upscaling from local flux measurements using biophysical models and remotely sensed information about vegetation activity.

[4] The experimental verification of the modeled CO_2 fluxes at the regional to continental scale represents a major scientific challenge [*IPCC*, 2001]. We study here regional scales of several hundreds of square kilometers where existing approaches comprise a so-called convective boundary layer (CBL) budgeting method and aircraft-based eddy covariance flux measurements. The latter give information on spatial patterns of carbon dioxide and water vapor fluxes

[1] Laboratoire des Sciences du Climat et de l'Environnement, UMR Commissariat à l'Energie Atomique/Centre National de la Recherche Scientifique 1572, Gif-sur-Yvette, France.
[2] Now at Condat-sur-Vienne, France.
[3] Institut für Chemie und Dynamik der Geosphäre II, Forschungszentrum Jülich, Jülich, Germany.
[4] MetAir AG, Hausen am Albis, Switzerland.
[5] Institut National de la Recherche Agronomique–Bioclimatologie, Villenave d'Ornon, France.
[6] Department of Plant Ecology, University of Bayreuth, Bayreuth, Germany.
[7] Now at Department of Forest Resources and Environment, University of Tuscia, Viterbo, Italy.

0148-0227/04/2003JD004335

across transects of several tens of kilometers [*Crawford et al.*, 1996; *Desjardins et al.*, 1982, 1997; *Ritter et al.*, 1994; *Gioli et al.*, 2004]. The CBL budgeting method assumes perfect mixing in the BL during daytime in order to obtain spatially integrated fluxes over horizontal scales of tens to hundreds of kilometers [e.g., *Denmead et al.*, 1996; *Laubach and Fritsch*, 2002; *Lloyd et al.*, 2001, 1996; *Raupach et al.*, 1992]. The essence of the method is to obtain the surface flux from measurements of the temporal change in the CO_2 mixing ratio in the CBL and information on exchange with the free troposphere (FT) aloft, using surface measurements, tall towers, tethered balloons, aircraft vertical profiles or combinations of these.

[5] Most investigations [e.g., *Denmead et al.*, 1996; *Levy et al.*, 1999] employed a Eulerian framework, with the assumption of stationarity and horizontal homogeneity, i.e., ignoring the advection of variable CO_2 mixing ratios to the observation site. In order to consider horizontal advection *Lloyd et al.* [2001] attempted to apply a quasi Lagrangian approach by moving the aircraft-based vertical profiles according to the forecasted mean wind. In another experiment, large-scale CO_2 advection was estimated from local profile information above the CBL [*Laubach and Fritsch*, 2002]. The influence of advection remains a central source of uncertainty in the Eulerian CBL budgeting approach, as heterogeneous land cover and upwind anthropogenic emission sources can produce sufficiently large horizontal variability in the atmospheric CO_2 mixing ratio to outweigh the changes due to surface fluxes. For instance, taking the temporal variability recorded at continuous CO_2 stations as an indicator of the spatial (horizontal) variability of CO_2 within an air shed in Europe suggests variations of up to 10–20 ppm across distances of a few hundreds of km [*Biraud et al.*, 2000; *Schmidt et al.*, 1996].

[6] Besides the advection of varying CO_2 mixing ratios into the experimental region, an important problem to overcome in populated areas is that the overall CO_2 flux within the concerned region is formed by the superposition of the biogenic CO_2 surface flux and CO_2 emissions from fossil fuel combustion sources. In order to determine the biogenic CO_2 fluxes correctly, it is thus essential to accurately account and possibly subtract the contribution of anthropogenic emissions. Carbon monoxide (CO), which is coemitted with CO_2 during combustion processes such as fossil fuel and biomass burning, is a valuable tracer to distinguish anthropogenic from biogenic surface fluxes, provided that biogenic sources of CO remain small and that over the experiment domain chemical reactions producing and destroying CO can be neglected [*Bakwin et al.*, 1998; *Gerbig et al.*, 2003; *Meijer et al.*, 1996; *Potosnak et al.*, 1999].

[7] In this paper we prove the concept of a novel Lagrangian approach to determine regional-scale CO_2 fluxes from airborne measurements of CO_2, CO and meteorological parameters aboard a small research aircraft. The experimental approach, based on an air mass following flight pattern to get rid of advection influences and the use of CO as tracer for anthropogenic CO_2 emissions, aims on the development of a method that should be applicable under more heterogeneous conditions preponderant in Europe. However, the campaign described in this paper was conducted over a "simple" region with a productive homogeneous forest, flat terrain, and without strong anthropogenic sources. This experiment under optimal conditions allows us to test the robustness of the method to constrain biogenic CO_2 fluxes. The CO measurements are here primarily used to verify the absence of locally or regionally polluted air. Additionally, starting from the experiment, the general usefulness of CO as a tracer to correct for anthropogenic CO_2 sources at regional scales is discussed, thus yielding the basis for future use of the experimental approach over more heterogeneous areas.

[8] The regional flux estimate derived from the aircraft experiment is compared with the local fluxes measured by eddy covariance on a tower located in the same forest and with a model estimate of regional net ecosystem exchange (NEE) based on remote sensing information.

2. Experimental Procedure

[9] The campaign was conducted in the "Landes de Gascogne" region, a very large forest of about 1.3×10^6 ha in the southwest of France (see Figure 1). The region was selected because of the size, homogeneity and high biological productivity of the forest, the existence of an eddy covariance tower with perennial meteorological and CO_2 flux measurements, the long-term climatological record available from the Bordeaux airport, and the meteorologically simple topographic situation. The investigation was made in June when the biological productivity is high.

[10] The Landes region is covered with monotype maritime pine forest (*Pinus pinaster*). The understory consists mostly of grass (mainly *Molinia caerulea* L. (Moench)) and the soil is a sandy hydromorphic podzol. Sparsely distributed in the forest are patches of agricultural fields (mainly maize). The climate is oceanic, characterized by mild temperatures (annual mean of about 13°C) and high precipitation (about 900 mm yr^{-1}) distributed all over the year with maximum in fall and winter. The area is flat (mean altitude about 50 m) and the dominant wind direction is SW. The area is exempt of significant anthropogenic sources, except for the city of Bordeaux in the North and the A63 motorway roughly parallel to the coast.

[11] The eddy covariance flux measurement site "Le Bray" [*Berbigier et al.*, 2001] is located in the same forest at (44°42′N, 0°46′W), about 30 km north of the area chosen for the Lagrangian experiment. The Bray site is equipped with a 40 m high tower, where, among others, NEE is measured by eddy covariance.

[12] Radio soundings of temperature and water vapor were obtained for the flight days from Météo-France at the nearby airport of Bordeaux (44°49′N, 0°41′W). During the campaign, additional soundings were made at 1000 UT and 1600 UT, in addition to the regular soundings at 1200 UT.

[13] The airborne measurements were carried out with a double-seated Super-Dimona, operated by MetAir AG. This small aircraft is equipped with instruments to measure a suite of chemical tracers (CO_2, CO, O_3, NO_2, NO_x, NO_y, PAN, O_x, C_4–C_{10} hydrocarbons and aerosols) and meteorological parameters. A detailed description of the aircraft and its instrumentation can be found in [*Neininger et al.*, 2001]. For this paper the analysis concentrates on the measurements of CO_2 and CO (online and flask samples),

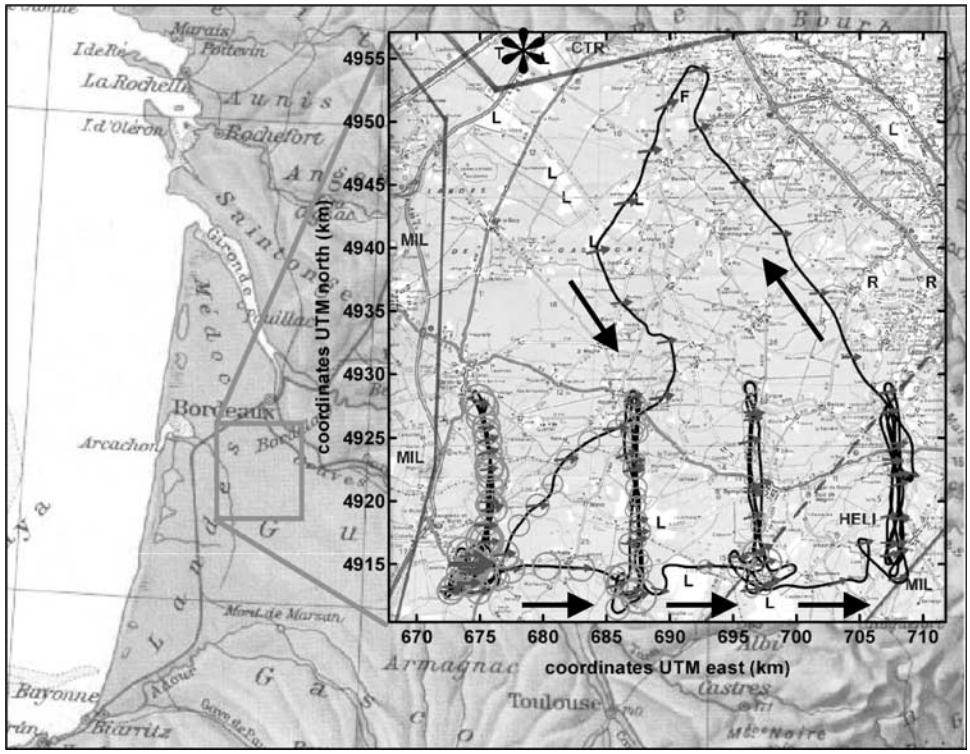

Figure 1. Map showing the location of the study area in southwest France. The zoom shows the track of the flight on 23 June 2001. Coordinates are given as km in Universal Traversor Mercator (UTM) (zone 30). Black arrows give the direction of the flight path, and shaded arrows give the wind direction. The circles correspond in size to the measured CO_2 mixing ratios. The asterisk in the upper left corner of the zoom area shows the position of the eddy flux tower "Le Bray." See color version of this figure in the HTML.

and meteorological parameters (temperature, dew point, pressure, three-dimensional (3-D) wind), which are briefly described in the following.

[14] The determination of meteorological parameters is made with a fine thermocouple and a miniature dew point mirror (Meteolabor TP-3, 1 Hz resolution). In addition, water vapor is measured at 10 Hz with an open path IR sensor (NOAA, IRGA). The advanced 3-D wind-sensing system consists of the following components: the flow angles are derived from a five hole probe equipped with differential pressure sensors (Keller); attitude and acceleration of the aircraft are obtained from a multiantenna, carrier phase sensitive GPS receiver (Trimble TANS Vector) and three accelerometers (Kistler). The inaccuracy of the deduced wind speed is less than ± 0.5 m s^{-1}.

[15] Carbon monoxide is measured by vacuum UV resonance fluorescence [*Gerbig et al.*, 1999; *Volz and Kley*, 1985], using a commercial instrument (Aerolaser AL-5003) manufactured under license of the Forschungszentrum Jülich GmbH. The instrument combines fast time response (5 Hz) with high precision (2 ppb or 2% at 1 Hz). The pressure-regulated inlet provides stable operation at ambient pressures down to 200 mbar. To avoid interference by atmospheric water vapor the sampled air is dried with $CaSO_4$. In-flight calibration of the instrument was made by overflowing the inlet with a cartridge containing about 1 ppm CO in synthetic air, which was calibrated at the ground against a primary standard (1 ppm CO in zero air, Messer Griesheim). A comparison of the primary standard at MPI Mainz yielded a mixing ratio of 971 ± 10 ppb CO (C. A. M. Brenninkmeijer, personal communication, 2001). For determination of the instrumental background signal, the in-flight standard was passed through a bed of Hopcalite, which quantitatively removed the CO to levels of <1 ppb. Calibration and zero adjustment were performed every 10 min with a duration of 45 s and were linearly interpolated in between. The overall inaccuracy of the 1 Hz CO mixing ratios was ±3 ppb or 3%.

[16] CO_2 is measured with a modified infrared gas analyzer (LICOR, LI-6262). The design of the commercial instrument is not sufficient for precise and accurate measurements aboard aircraft because of the influence of changing pressure and temperature. The few existing high-accuracy aircraft instruments are therefore enclosed in completely temperature and pressure stabilized environments and are operated with in flight calibration standards in order to achieve an accuracy of 0.1–0.2 ppm during flight, [cf. *Daube et al.*, 2002; *Filippi et al.*, 2003]. As these designs were too large and heavy for the limited payload and volume of our platform we tried to improve the accuracy of the LI-6262 without excessively increasing the volume and weight. The following modifications were made.

[17] The outlets of measurement and reference cells were connected downstream in order to balance the pressures in both cells, and a heat exchanger between the intakes of

measurement and reference cells served to provide equal temperature in both cells. The temperature sensor was moved to the outlet of the measurement cell in order to capture fast changes. The reference cell was continuously flushed with a CO_2 mixture (360 ppm in air), which increases the precision and decreases the influence of errors in temperature and pressure measurements by about a factor of 10. The reference gas was taken from a lightweight gas cartridge at a flow rate of 20 mL min^{-1} (STP). The sample gas was supplied to the instrument at a flow rate of 350 mL min^{-1} by means of a membrane pump (KNF-Neuberger, EPDM membrane), which was tested at IUP-Heidelberg for suitability with regard to CO_2 measurements. The sample air was dried with magnesium perchlorate, which was placed upstream of the pump. In this configuration any possible bias caused in the CO_2 mixing ratios due to the influence of magnesium perchlorate under changing pressure should be smaller than 0.25 ppm [*Levin et al.*, 2002]. The in situ CO_2 mixing ratios were recorded at a frequency of 1 Hz, although the effective temporal resolution due to the gas mixing in the absorption cell ($\sim$10 mL volume and $\sim$5 mL s^{-1} flow rate) was only 0.2–0.5 Hz.

[18] Instead of deploying in-flight calibration gases, the accuracy of the in situ CO_2 measurements was validated against 8–12 flask samples collected during each flight into preconditioned 1 L glass flasks equipped with two PFA O-ring valves. The flasks were filled during horizontal sections of the flight legs and were flushed for more than 5 min at a flow rate of about 4 L min^{-1} before being pressurized to about 1 bar above ambient pressure at final filling. The flask sampling system was connected to the sampling line of the LICOR downstream of the pump. Twenty-four flask samples were analyzed at the Laboratoire des Sciences du Climat et de l'Environnement (LSCE), and 15 (taken on 23 June and part of the flight of 25 June) were analyzed at the IUP. At both laboratories, CO_2 was measured by custom build gas chromatography systems (GC-FID) with a precision better than 0.1 ppm [*Levin et al.*, 2002; *Pépin et al.*, 2001]. A small correction for a drift in the CO_2 mixing ratio during storage of the flasks was applied (+0.15 ppm for the LSCE flasks, 75 days storage, and +0.09 ppm for the IUP flasks, 23 days storage), on the basis of tests described by *Levin et al.* [2002].

[19] Comparison of the online CO_2 measurements with flask samples (see below) has revealed a systematic bias in the mixing ratios of up to 1 ppm for level runs and 2 ppm for profiles. Further tests showed that the problems were caused by (1) a small temperature dependence of the CO_2 mixing ratio in the reference gas cartridge and (2) leakage of outside air into the chopper and sensor housing of the LICOR together with an insufficient efficiency of the factory installed CO_2 scrubber. For cause 1, laboratory tests yielded an experimental factor of 0.08 ppm(CO_2)/K, which was used to correct the in situ measurements. To correct for cause 2, four parameters were defined in a semiempirical model describing the exchange with outside air in the chopper housing due to pressure differences and diffusion: a time constant; a pressure offset to describe diffusion without pressure difference; an efficiency factor giving the influence on the measurement; and a maximum error to exclude extreme corrections. These parameters were optimized including additional data from later flights where the problem was investigated in more detail, before finally being solved by flushing the optics of the LI-6262 with synthetic air. The remaining inaccuracy of the thus corrected data depends on the actual flight patterns, including ascent/descent rates, and the vertical structure of the atmosphere. It is ±0.3 ppm for the level flights on 23 June and deteriorates up to ±1 ppm for individual vertical profiles.

[20] The mean difference between the corrected in situ CO_2 measurements and the flask samples was 0.0 ± 0.4 ppm and 0.7 ± 0.1 ppm for the flasks analyzed by LSCE and IUP, respectively. The resulting mean difference between LSCE and IUP was larger than that found in regular intercomparisons between the two laboratories (0.28 ± 0.15 ppm bias [*Levin et al.*, 2003]). A possible explanation might be the longer storage time of the flasks analyzed by LSCE. Most important for the evaluation of the Lagrangian experiment, however, is the stability of the LI-6262 measurements during each flight, as given by the standard deviation of the comparison between the in situ data and the flask analysis. For 23 June the standard deviation of the comparison with the flasks analyzed by IUP is ±0.1 ppm, i.e., three times better than the a priori estimate of the accuracy for this day.

[21] The flask samples were also analyzed for CO at LSCE using a commercial GC analyzer (Trace Analytical RGA3, overall uncertainty 4% [*Gros et al.*, 1999]). The mean difference between in situ measurements and flask analysis was -3 ± 4 ppb, well within the estimated accuracy of the measurements, the standard deviation being largely explained by the imprecision of the GC analysis.

3. Results

3.1. Observations

[22] The campaign consisted of four flight days as summarized in Table 1. The sampling strategy was to determine the mean mixing ratio of CO_2 and CO in the CBL by flying a stack of horizontal legs perpendicular to the wind direction. The stacks were repeated at a distance determined from the mean wind speed in order to intercept the same air mass at consecutive stacks. Depending on the actual BL height, each stack consisted of two to three equally spaced altitude levels. Each horizontal leg was flown twice in opposite directions so that time derivatives approximately cancel [*Betts et al.*, 1992]. In order to obtain information on the vertical structure of the CBL and the FT aloft, vertical profiles from around 50 m above ground into the FT were flown at each stack. In addition, the radio soundings obtained from Météo-France at the Bordeaux airport where used to characterize the BL top.

[23] On three of the days, 21, 22, and 25 June 2001, anticyclonic conditions prevailed, favoring the development of large local eddies and the entrainment of free tropospheric air (Table 1). Low wind speeds in conjunction with large variability in wind direction did not allow an appropriate planning of the Lagrangian flight patterns. The observations showed a strong spatial variability in the CO and CO_2 mixing ratios, reflecting the varying contributions of anthropogenic emissions and entrainment from the FT. The Lagrangian approach was hardly applicable in those situations.

Table 1. Meteorological Conditions During the COCA Flights at the Bray Site, Bordeaux, in June 2001

Date	Time of Flight, UT	Experimental Area, deg	Synoptic Conditions	Wind Direction,[a] deg	Wind Speed,[a] km h^{-1}	Maximum Ground TT, °C	Clouds	Boundary Layer Height, m	Boundary Layer Characteristics	Technical Remarks	Suitable for Lagrangian Estimates?
21 June	1246–1714	44.15–44.5N, 0.62–0.82W	anticyclonic	340 ± 40, variable in space and time	12 ± 5	31.0	clear skies	1400–1700	Decreasing BL height with time. BL getting more stable with time.		no
22 June	1126–1546	44.2–44.5N, 0.62–0.8W	anticyclonic	321 ± 66, very variable in space and time	7 ± 2	31.6	clear skies	1300–1700	Wind direction highly variable in space and time. Increasing BL height during flight. BL slightly stable during the flight.		no
23 June	1155–1452	44.35–44.48N, 0.4–0.8W	cyclonic	261 ± 8	19 ± 1	23.1	low scbase at ~750 m asl	~700	Constant cloud base BL height assumed to be steady. Strong inversion layer above 670 m. From ground to ~250 m well mixed, above slightly stable stratification. No entrainment from free troposphere possible.	CO_2 drying system saturated after 1410 UT.	yes
25 June	1126–1605	44.2–44.5N, 0.45–0.85W	anticyclonic	130 ± 38, very variable in space and time	6 ± 2	34.6	clear skies	750–1100	Strong vertical wind shear. Increasing BL height during flight, with a breakdown during the last stack.		no

[a]Within convective boundary layer.

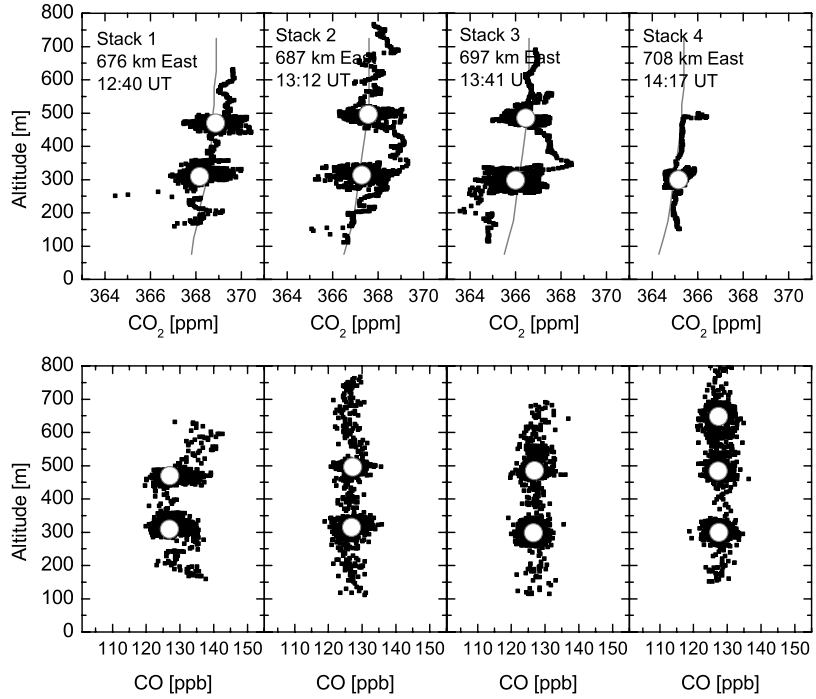

Figure 2. Vertical profiles of (top) CO_2 and (bottom) CO mixing ratios for the four stacks of the flight on 23 June 2001. Black dots give 1 s data, and white circles give the mean mixing ratio for each altitude level. The gray lines display the vertical CO_2 profiles calculated with a one-dimensional Lagrangian model (see text for model details). The mean position in UTM and the mean time for each stack are given in the graphs.

[24] In the following we concentrate on the flight conducted on 23 June 2001, a day with well-defined meteorological conditions (compare Table 1). Figure 1 shows the flight track overlaid on a map of the area. The average wind direction was west (261° ± 8°). The flight pattern consisted of four stacks extending about 15 km in north-south direction and displaced by 11 ± 1 km in west-east direction. Each stack was composed of two horizontal level runs flown at altitudes of about 300 m and 500 m, respectively. Because of the low mixing layer height, as indicated by the base of the stratocumulus clouds at 700 m, only two altitude levels were flown. The time difference between two consecutive stacks was 32 ± 3 min, in good agreement with the time difference of 35 min ideally required for fulfilling the Lagrangian condition, according to the measured average wind speed. For the last stack a third altitude level at ~700 m had been added. Unfortunately, the $MgSO_4$ drying cartridge saturated during that part of the flight, so that the corresponding CO_2 measurements are subject to larger errors and hence were not included in the analysis.

[25] Vertical profiles of CO_2 and CO for the different stacks are shown in Figure 2 and the mixing ratios measured along the horizontal legs are shown in Figure 3. The mean mixing ratio from each horizontal leg is marked by a white circle. The CO mixing ratios in the BL showed variations of less than ±5 ppb during the entire flight. The average differences between consecutive stacks were <1 ppb. Only at the southern edge of the first stack and during sampling the vertical profile at the same position slightly higher CO mixing ratios (about 10 ppb) were observed. This points to a slight anthropogenic influence at the edge of the flight area. Although this influence is relatively small, the corresponding part is excluded from all stacks in the budget analysis. The resulting domain for the budget has an area of 230 km^2.

[26] The CO_2 mixing ratio shows variations of about 2 ppm within each profile, as well as along the horizontal flight legs. The CO_2 mixing ratios are anticorrelated with the water vapor mixing ratio (Figure 4) and the vertical wind component, indicating that these variations are due to air parcels depleted in CO_2 by photosynthesis and enriched in H_2O by evapotranspiration. On average, the CO_2 mixing ratio exhibits a monotonous decrease between subsequent stacks with a difference of about 3 ppm between the first and last stack, clearly indicating the uptake of CO_2 over the experimental area. Both, the vertical profiles and the mean mixing ratios of the horizontal flight legs show a decrease in CO_2 toward the surface with an average gradient of about 0.3 ppm CO_2 per 100 m, again reflecting the uptake by the biosphere.

3.2. CO_2 Budget

[27] The vertical gradients and the considerable variance of CO_2 apparent in the profiles (Figure 2) suggest a not perfectly mixed BL. On the other hand the correlations between CO_2, water vapor and the vertical wind component (Figure 4) point to the existence of large turbulent eddies, which averaged over the whole area should lead to a well mixed BL. Having these different observations in mind we estimate the CO_2 fluxes with two independent methods.

[28] First, we calculate the fluxes with a simplified time-dependent one-dimensional Lagrangian model. This model explicitly treats the vertical mixing by using the 3-D wind

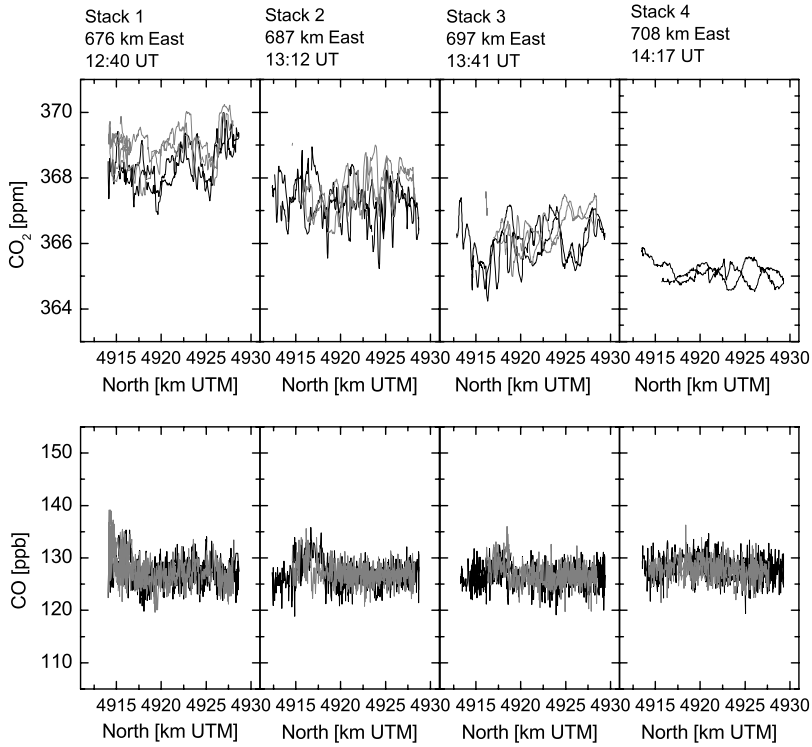

Figure 3. (top) CO_2 and (bottom) CO mixing ratios for the horizontal legs of the four stacks of the flight on 23 June 2001. Measurements at the lower leg (~300 m) are shown in black and at the upper leg (~500 m) in gray. The mean position in UTM and the mean time for each stack are given in the graphs.

measurements aboard the aircraft to estimate the strength of the vertical turbulence and allows to establish the mean vertical profile in the BL. The method also helps to easily calculate the influence of variable initial and boundary values on the CO_2 fluxes and hence their possible errors.

[29] Second, we apply the classical convective boundary layer budgeting approach (CBL approach) mentioned in the introduction, although the assumption of vertical homogeneity seemed to be not strictly fulfilled for our experiment. This analytical determination of the surface fluxes, once its validity is confirmed by comparison with the 1-D model results, allows a general analysis of uncertainties.

3.2.1. 1-D Model Estimate

[30] According to the continuity equation, the local rate of change of a scalar tracer is given by

$$\frac{\partial c_m}{\partial t} = P - L - \mathbf{u}\nabla c + \nabla K \nabla c. \qquad (1)$$

Here c is the local concentration of the tracer, $P - L$ is the net source term, $\mathbf{u}$ is the three-dimensional wind vector, and K is the three-dimensional eddy diffusion tensor. In the case of CO_2, which has no significant chemical sources or sinks in the BL, $P - L$ equals zero. For a Lagrangian experiment the following definitions and approximations hold: Since dx is oriented along the axis of advection after the coordinate transformation, the wind components equal zero on average. The diffusion term in the direction of advection ($Kxdc/dx$) can be neglected against advection and the experimental data demonstrate homogeneity in the y direction (Figure 3). Therefore diffusion in the y direction can be neglected and the integration over y can be replaced by the average concentrations of the different legs. With this we obtain for a Lagrangian coordinate system moving with the mean wind

$$\frac{dc_m}{dt} = \partial K_z(\partial c/\partial z)/\partial z = \partial K_z(\partial(\mu \cdot \rho)/\partial z)/\partial z, \qquad (2)$$

where z is the vertical coordinate, K_z is the vertical eddy diffusion coefficient, μ is the mixing ratio of the tracer, and ρ is the density of air.

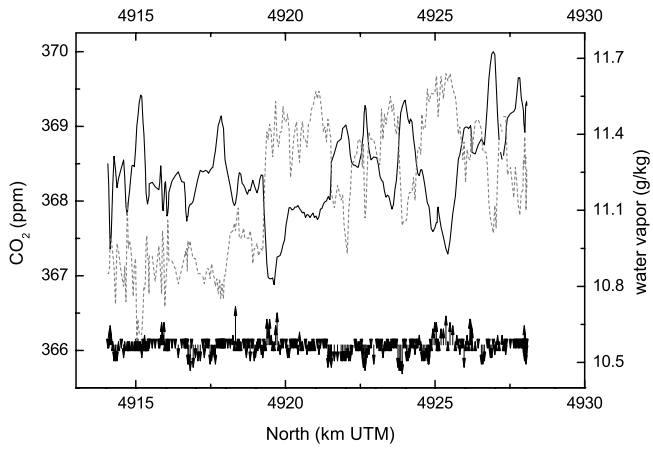

Figure 4. CO_2 (black line) and water vapor (dashed gray line) mixing ratios for the lower leg (~300 m) of the first stack of the flight on 23 June 2001. The vertical wind component is indicated by the black arrows.

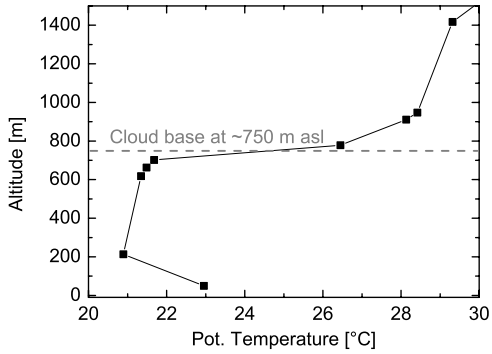

Figure 5. Potential temperature from a radio sounding at Bordeaux airport on 23 June 2001, 1200 UT (Météo-France). The dashed line gives the average altitude of the cloud base observed during the flight.

[31] Integration of equation (2) over z and t requires boundary conditions at the top and the bottom of the BL. These are the surface flux (F_c) at $z = 0$ and the exchange flux with the free troposphere (F_+) at $z = h$. Equation (2) was integrated numerically in a one-dimensional Lagrangian model, by calculating the rate of change in the CO_2 mixing ratio within a moving vertical column using an explicit finite difference scheme that included vertical mixing. The model was set up as follows.

[32] The vertical grid size was 50 m, equally spaced between the surface (50 m above sea level (asl)) and the top of the BL. As the dense stratocumulus cloud prevented the aircraft to enter the free troposphere for flight safety reasons, the BL height was determined from the radio sounding of Météo-France at 1200 UT at Bordeaux airport (Figure 5). The height of 700 m above ground (750 m asl) thereby derived is consistent with the altitude of the cloud base observed during the flight (650–700 m above ground during the flight time 1200–1430 UT). An additional box in the FT provided the upper boundary condition with a CO_2 mixing ratio of 372 ppm, adopted from the measurements in the FT on the other days of the campaign. The vertical eddy diffusion coefficient K_z was estimated from the variance of the 3-D wind measurements (u', v', w') aboard the aircraft according to equation (3) [*Stull*, 1988]:

$$K_Z = \mathrm{TKE}/|\partial\bar{U}/\partial z|, \tag{3}$$

with $\mathrm{TKE} = 0.5(\overline{u'^2} + \overline{v'^2} + \overline{w'^2})$ being the average turbulent kinetic energy and with $\partial\bar{U}/\partial z$ being the vertical gradient of the mean wind.

[33] Averaging of equation (3) over the profiles 4 and 6 from 110 to 610 m above ground yields a mean value of $K_z = 100 \pm 60$ m^2 s^{-1} for the boundary layer.

[34] The model was initialized with the data from the first stack and the surface flux F_c was determined in an iterative procedure by optimizing the horizontal CO_2 decrease to best fit the measurements made at the subsequent legs, which were sampled according to their respective distances. The conversion into time was made using the average wind velocities between the different stacks. The time step for integration was 3 s.

[35] In the first model run, the exchange coefficient between the uppermost BL box and the free troposphere K_{z+} was set equal to zero, because of the very strong temperature inversion of >2K/100 m topping the BL (see Figure 5) and hence suppressing vertical turbulence. The resulting vertical CO_2 profiles are displayed in Figure 2. The observed mean mixing ratios at the level runs are well reproduced by the model for all stacks. The deviations of the few data points in the vertical profiles are due to the poor representativeness in the measured data caused by the atmospheric variability within the BL. The required surface flux is $F_{CO_2} = -15.2$ μmol m^{-2} s^{-1}. Additional model runs were made in order to investigate the sensitivity to the assumptions for the upper boundary condition and the vertical eddy diffusion coefficient:

[36] The correctness of the upper boundary condition was investigated by initializing the model with a constant CO_2 profile of 372 ppm at the Atlantic coast. The model reproduced the mean mixing ratio measured at the first stack (368.5 ppm) with the same surface flux for the area between the coastline and the first stack as that derived from the differences between the stacks. As the CO_2 profile in the air advected from the ocean should be constant with height due to the absence of sources and sinks, this result confirms the assumption for the upper boundary condition.

[37] Changing the value for K_z from 100 to 40 and 160 m^2 s^{-1} changed the surface flux required to reproduce the horizontal gradient of 0.11 ppm km^{-1} by less than ±0.1 μmol m^{-2} s^{-1}, but produced a factor of two larger and smaller vertical gradients, respectively, than found in the measurements. Additional model runs were made allowing exchange with the free troposphere using K_{z+} = 0.5 m^2 s^{-1} and an extreme value of K_{z+} = 1 m^2 s^{-1}. The inferred CO_2 surface flux increased to −16 and −17 μmol m^{-2} s^{-1}, respectively. The fit to the observations was again within the uncertainty of the measurements. Finally, the uncertainty in the BL height produces a corresponding uncertainty in the CO_2 flux. In summary the 1-D model gives a surface flux of −16 μmol m^{-2} s^{-1} with a 1-sigma error of ±1.5 μmol m^{-2} s^{-1}.

3.2.2. Convective Boundary Layer Budget Approach

[38] The CBL approach in a Lagrangian coordinate system, as described, for example, by *Denmead et al.* [1996] and *Lloyd et al.* [2001], can be written as

$$\frac{d\mu_m}{dt} = \frac{F_c}{M_m} + \left(\frac{\mu_+ - \mu_m}{M_m}\right)\left(\frac{dM_m}{dt} - W_+\right). \tag{4}$$

The BL dimensions are expressed as moles of air per unit ground area, $M_m = \rho_m h$, where h is the BL height and ρ_m is the mean molar density of air in the BL. The variables μ_m and μ_+ are the average mixing ratios of the trace gas c in the BL and above the top of the CBL, respectively. F_c is the flux density of the tracer at the surface (in units of mol m^{-2} s^{-1}). The second term on the r.h.s. of equation (4) gives the entrainment from the free troposphere [*Laubach and Fritsch*, 2002]. It contains the potential increase in the BL height (dM_m/dt) and the entrainment by vertical advection ($W_+ = \rho_+ w_+$, with ρ_+, w_+, air density, vertical wind speed at top of the CBL). The latter is defined positive when pointing upward and must be balanced by a corresponding divergence in the

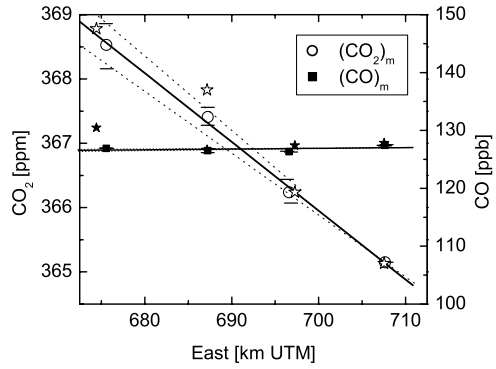

Figure 6. Mean mixing ratios of CO_2 (open circles) and CO (filled squares) for each stack of runs plotted over the coordinates in wind direction (east). The horizontal bars show the individual means for the lower and upper runs. The stars (open, CO_2; filled, CO) show the mean mixing ratios as estimated from the vertical profiles. The solid lines give the linear fit for the stack means; the dotted lines give the linear fit for the lower and the upper runs separately.

horizontal wind field. Rearranging of equation (4) yields the surface flux:

$$F_c = M_m \frac{d\mu_m}{dt} - (\mu_+ - \mu_m)\left(\frac{dM_m}{dt} - W_+\right). \quad (5)$$

F_c is derived from the observed temporal change in μ_m and M_m as determined by a minimum of two measurements at two different times. Integration of equation (5) yields

$$\langle F_c \rangle = \frac{1}{\Delta t}\int_{t_0}^{t_1} F_c dt = \frac{(M_m(t_1) - \langle W_+ \rangle \Delta t)\cdot(\mu_m(t_1) - \langle \mu_+ \rangle) - M_m(t_0)\cdot(\mu_m(t_0) - \langle \mu_+ \rangle)}{\Delta t}, \quad (6)$$

with angle brackets denoting average values. The time period Δt between the observations is calculated from their horizontal distance and the mean wind speed.

[39] For the simple case of a constant BL height, as suggested by the observations, and neglecting divergence in the horizontal wind field ($w_+ = 0$), equation (6) simplifies to

$$\langle F_c \rangle = \frac{\langle M_m \rangle \cdot (\mu_m(t_1) - \mu_m(t_0))}{\Delta t}. \quad (7)$$

The mean BL mixing ratio is estimated from the mean mixing ratios of the horizontal traverses at the two altitude levels (300 and 500 m), with a minor correction of −0.05 ppm for the vertical gradient derived from the 1-D model.

[40] Figure 6 shows the mean mixing ratios of CO_2 and CO for each stack plotted against the downwind distance, $\Delta x = \langle v_x \rangle \cdot \Delta t$. The decrease in the CO_2 mixing ratio between the four stacks is well described by a linear fit. The large correlation coefficient ($r^2 = 0.99$) of the relationship between μ_m and Δx suggests that F_{CO_2} was approximately constant over the experiment and that the Lagrangian conditions were fulfilled at very good approximation. In other words,

$$\langle F_c \rangle = \langle M_m \rangle \cdot \langle v_x \rangle \cdot \frac{\Delta \mu_m}{\Delta x}. \quad (8)$$

From the slope of the regression ($d\mu_m/dx = -0.107$ ppm km^{-1}), the average wind speed (19 km h^{-1}) and the BL height (700 m), an average regional CO_2 flux of $\langle F_{CO_2} \rangle = -16$ μmol m^{-2} s^{-1} is derived from equation (8) over the experimental domain, in excellent agreement with the results from the 1-D model above.

3.3. Uncertainties

[41] Table 2 summarizes the various errors that contribute to the overall uncertainty in $\langle F_{CO_2} \rangle$. Random errors due to the variability in **u** and CO_2 vanish after integration over the entire domain. The systematic error of ΔCO_2 due to potential drift in the sensitivity of the LICOR instrument is ±0.3 ppm for the level flights on this day. The systematic error on the wind speed for the flight patterns with forward and backward legs is ±0.3 m s^{-1} (1 sigma) The corresponding uncertainty in the horizontal gradient is ±0.013 ppm km^{-1}. Including the uncertainty in M_m arising from the uncertainty in the BL height (Δh = ±50 m), the experimental (1 sigma) uncertainty in the CO_2 flux is ±12.5% or ±2.0 μmol m^{-2} s^{-1}. Additional sources of errors arise from the various assumptions made in the CBL budget equation or the 1-D model.

Table 2. Sources of Error and Their Influence on the Uncertainty of $\langle F_{CO_2} \rangle$

Type of Error	Remarks	Error Estimates	Corresponding Uncertainty of $\langle F_{CO_2} \rangle$, μmol m^{-2} s^{-1}
Experimental uncertainty	Error propagation (1 sigma)	$\Delta[CO_2]$ = ±0.3 ppm Δv_x = ±0.3 m s^{-1} Δh = ±50 m	±2.0
Representativeness error	Uncertainty of average CO_2 due to imperfect sampling of the BL	Mean error from values for individual stacks and legs (see Table 3)	±1.1
Methodical error	Uncertainty of exchange with FT	Estimated alternatively from uncertainty in k_{z+} and the entrainment term in the CBL budget (see text)	±1
Uncertainty of anthropogenic CO_2 flux $\langle F_{CO_2} \rangle_a$	Estimated from uncertainty of CO flux	$\Delta[CO]$ = ±2.5 ppb	±0.5

Table 3. $\langle F_{CO_2} \rangle$ From Equation (8) for Different Flight Areas and Methods of Determination of $[CO_2]_m$[a]

	Stack Means	Lower-Level Means	Upper-Level Means	Profile Means
Area between stack 1 and 2	−14.5	−11.5	−16.6	−14.9
Area between stack 2 and 3	−18.5	−18.9	−17.9	−23.9
Area between stack 3 and 4	−14.3	−12.6		−15.7
Average over total area[b]	−15.6	−14.1	−17.2[c]	−17.9
Average over total area[d]	**−16.0**	**−14.7**	**−17.0**	**−19.0**

[a]Fluxes $\langle F_{CO_2} \rangle$ are given in μmol m^{-2} s^{-1} (negative numbers signify uptake of CO_2).
[b]$\langle F_{CO_2} \rangle$ = area weighted mean of the fluxes for each stack area.
[c]Likely biased high due to missing information for stacks 3 and 4.
[d]$\langle F_{CO_2} \rangle$ from linear fit.

[42] The Lagrangian approach requires the subsequent measurements to be made within the same air mass. In our experiment, the time between the measurements differed by 10% from the travel time of the air between the stacks. This slight deviation from the Lagrangian condition is negligible for the conditions on 23 June when a homogeneous air mass was advected from the Atlantic ocean, since the time difference in the analysis was calculated from measured wind speed and distance, instead of the actual flight time between the measurements.

[43] The error of the average CO_2 flux due to incomplete sampling (representativeness error) can be estimated from the mean error of the fluxes calculated separately from the lower and upper legs and for the areas between the individual stacks. It amounts to ±7%. The fluxes between the stacks are constant within the uncertainties due to experimental errors and are similar to the average flux over the whole domain obtained from the linear fit over all stacks (see Figure 6 and Table 3).

[44] It should be pointed out that the fluxes derived from the changes in vertical profiles only (also included in Figure 6 and Table 3) show much larger variance. For instance, the flux between stack 2 and 3 would then be almost twice as large as the flux between stack 1 and 2 or stack 3 and 4, leading to an uncertainty of ±20%. This clearly questions the representativeness when only a few vertical profiles are used for flux estimations [e.g., *Laubach and Fritsch*, 2002; *Lloyd et al.*, 2001].

[45] A potentially large error comes from insufficient knowledge of the entrainment term or the turbulent exchange with the free troposphere. The results for the minimum and maximum value for K_{z+} in the 1-D model yields an uncertainty of the CO_2 flux of ±1 μmol m^{-2} s^{-1}. Alternatively, this error can be estimated from the entrainment term in the CBL approach. With $\langle CO_2 \rangle_m$ = 366.8 ppm (average over all stacks), $[CO_2]_+$ = 372 ppm and an increase in h of 50 m (according to the uncertainty in the BL height), the corresponding CO_2 increase in the CBL is (372−366.8) ppm × 50 m/700 m = 0.37 ppm.

[46] If we add this to the total CO_2 decrease over the domain (3.5 ppm), the surface flux $\langle F_{CO_2} \rangle$ is increased by 11% to an uptake of 18 μmol m^{-2} s^{-1}. On the other hand, a mean upward wind w_+ of ∼40 m h^{-1} is suggested by a meteorological forecast for the region based upon the ECMWF analysis for 1200 UT (F. Chevallier, personal communication, 2003). According to equations (5) and (6) this upward flux would basically compensate the effect of an increasing BL height on the surface flux. This can be discussed further:

[47] Under the prevailing meteorological situation with the BL being capped by a stratocumulus cloud layer the BL height is unlikely to rise [*Stull*, 1985] and the reliability of the vertical wind component in the ECMWF analysis has been questioned in several publications [e.g., *Stohl and Koffi*, 1998].

[48] As stated earlier, an upward motion would have to be sustained by a convergence in the horizontal wind field, or a decrease in the mean wind speed, respectively. The measurements indeed suggest a decrease in the mean wind speed along the axis of advection of about 2 km h^{-1} between the first and last stack. Yet, the data also suggests a slight divergence in the horizontal wind field of the order of 5°, which would compensate for the decrease in wind speed, thus yielding $w_+ \approx 0$. However, when neglecting the rather uncertain angular component of the horizontal divergence and attributing the change in wind speed solely to w_+, the value estimated from the ECMWF analysis is basically confirmed and the magnitude of the surface flux would increase by 6% to −17 μmol m^{-2} s^{-1} (note one half of the change in **u** over the domain is already accounted for by using the average wind speed for the budget calculation).

[49] Finally the potential error due to the presence of anthropogenic sources on the CO_2 budget is estimated from the CO data as follows. The average change in the CO mixing ratios was $d[CO]_m/dx$ = 0.01 ± 0.02 ppb km^{-1}, giving a CO flux $\langle F_{CO} \rangle$ = 1.5 ± 11 nmol m^{-2} s^{-1}. The uncertainty is dominated by the inaccuracy of the instrument. Entrainment and vertical motion can be neglected for CO, as there is no flux on which it could act and because the mixing ratio of CO in the FT is similar as in the BL due to advection from the Atlantic. With an anthropogenic CO/CO_2 emission ratio of 22 ppbCO/ppmCO_2, adopted from the 1995 emission inventory (see CITEPA, Emissions dans l'air en France: Emissions de certaines substances en 1995 dans les departements de la metropole, 2001, http://citepa.org) for the "Landes" department which includes the flight area, the corresponding anthropogenic CO_2 flux is $\langle F_{CO_2} \rangle_a$ = 0.1 ± 0.5 μmol m^{-2} s^{-1}. The uncertainty of the CO derived anthropogenic CO_2 flux amounts to 3% of the total CO_2 flux, which is negligible when compared to the other sources of error. In summary of the above sources of uncertainties, by propagation of all instrumental and methodical errors (see also Table 3), we arrive at a best estimate for the surface biospheric uptake of 16 ± 2.5 μmol m^{-2} s^{-1} with 95% confidence limits of 11 and 21 μmol m^{-2} s^{-1}.

4. Discussion

4.1. Comparison of the Regional Lagrangian CO_2 Flux With Eddy Covariance and Satellite-Based Estimates

[50] Figure 7 shows the comparison of the CO_2 flux (NEE) from the Lagrangian experiment with the local CO_2 flux measured at the Bray tower (footprint ∼1 km^2) at the time of the experiment. The results of this comparison are summarized in Table 4. The NEE estimate from the regional budget is about 15% lower than the local NEE measured by eddy covariance at Le Bray, well within the combined uncertainties of the two measurements.

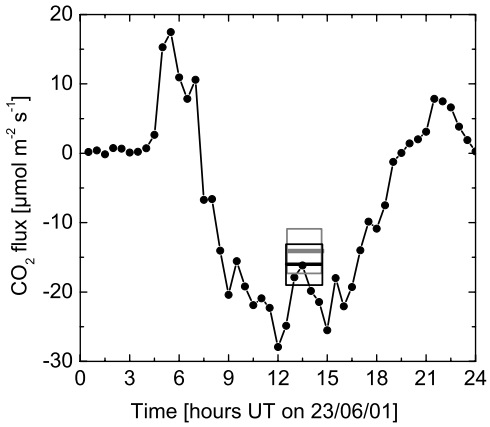

Figure 7. Net ecosystem CO_2 exchange (NEE) from the eddy correlation measurement at the "Le Bray" tower on 23 June 2001 (circles). The black bar shows the regional NEE from the Lagrangian convective boundary layer budget, and the gray bar shows the regional NEE modeled via remote sensing input (the boxes indicate the 1-sigma uncertainties, as in Table 4).

[51] Also shown in Figure 7 is the regional average NEE over the flight domain predicted by a biophysical model. The details of the computation procedure are presented in Appendix A. Briefly, a radiation use-efficiency model, driven by data from the Moderate-Resolution Imaging Spectroradiometer (MODIS) data stream (at 1 km resolution) on the incident radiation and the fraction of absorbed photosynthetic radiation, was used to estimate daily values of gross primary production (GPP). For the comparison, the modeled daily GPP was converted to NEE over the time interval of the flight using an empirical relationship established from the covariance flux measurements at the tower.

[52] The model-based estimate of average NEE for our experimental area is about 12% lower than the result from the Lagrangian experiment. The deviation is smaller than the uncertainty in the experimental data and of similar magnitude as the uncertainty in the conversion of modeled GPP to NEE.

[53] The model provides a link for the comparison between the regional flux derived from the Lagrangian flights and the local flux at Le Bray, which, a priori, lacks significance because of the poor spatial representativeness of a local flux measurement. The remote sensing data suggests, however, that the modeled NEE is rather homogeneous over a large portion of the flight domain with an interquartile range of less than 3 µmol m^{-2} s^{-1} (compare Figure A1), and also suggests that the modeled NEE in the flight domain is only 4% lower than the modeled NEE at the tower (compare Table 5). Thus the good agreement of the Lagrangian regional NEE estimate with the local flux at Le Bray is indeed a strong support for the validity of the Lagrangian budget.

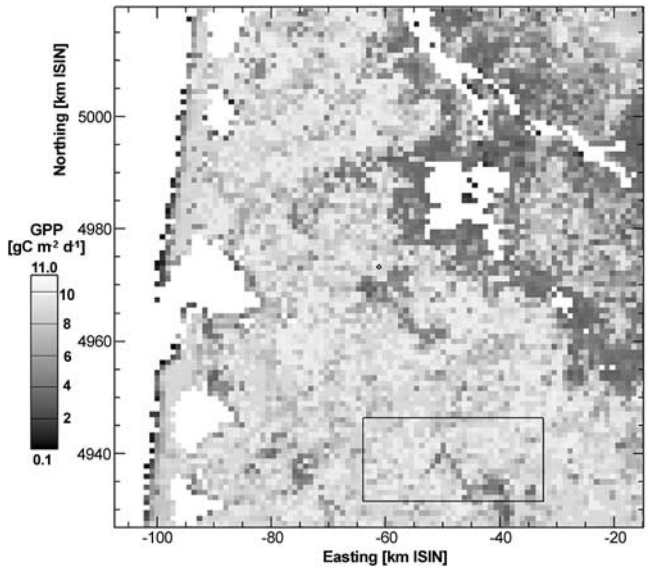

Figure A1. Map showing the estimated spatial gross primary production (GPP) distribution centered around the Bray tower site. The dot represents the tower site location, while the rectangle denotes the flight area over which the GPP estimates have been averaged. Shading encodes the amount of GPP according to the legend on the left. White pixels are not computed (water bodies or urban). The projection is the Integerized Sinusoidal (ISIN) that is used for Moderate-Resolution Imaging Spectroradiometer (MODIS) products. See Appendix A for details on the calculation.

4.2. Use of CO as a Tracer for Anthropogenic CO_2 Fluxes

[54] CO was successfully used to verify the absence of significant anthropogenic CO_2 emissions within the experimental area. The general usefulness of CO as a tracer to correct for anthropogenic CO_2 sources needs some further consideration.

Table 4. Comparison of Observed and Modeled Daily Gross Primary Production (GPP) and Flight Time Net Ecosystem Exchange (NEE) for the Tower Site and the Flight Area[a]

	Le Bray Tower		Flight Area	
	Observed Via Eddy Covariance	Modeled Via Remote Sensing Input[b]	Observed Via Lagrangian Budget	Modeled Via Remote Sensing Input[b]
Daily GPP, gC m^{-2} day^{-1}	9.4 (1.4[c])	8.8 (1.9)		8.6 (1.9)
NEE (1230–1430 UT), µmol m^{-2} s^{-1}	−18.8 (3.3[c])	−14.6 (3)	−16 (2.5)	−14.1 (3)

[a]Error estimates (1-sigma) are indicated in parentheses.
[b]See Appendix A for details.
[c]Propagated from the random error of the observations (7%), the systematic error (15%), and the temporal variations during the flight time (standard error).

[55] The CO contribution from combustion sources adds to the global background (~40 ppb) produced from the oxidation of CH_4. Natural CO emissions include a small source from oceans and plants, and the oxidation of biogenically emitted hydrocarbons, such as isoprene and terpenes. On a global scale, the latter source is of similar magnitude as the fossil sources [*IPCC*, 2001]. On experimental time scales of a few hours, however, this contribution is expected to remain small even when assuming a high estimate of the net production rate of CO of 1.2 ppb h^{-1}, as derived from measurements in a pine forest in central Greece [*Gros et al.*, 2002]. The major loss pathway of CO in the atmosphere is via reaction with OH radicals (a very small proportion is also lost by microbial uptake in soils). Using a high estimate for the OH concentration (10^7 cm^{-3}), the photochemical sink of CO is less than 0.1% h^{-1}, again negligible over experimental time scales of a few hours (assuming 200 ppb CO, the loss would be less than 0.5 ppb in 2 h). Once integrated over the duration of the experiment, the net effect of oxidation of biogenic VOC and loss by OH, would thus be less than 2 ppb, which is just at the detection limit of the CO instrument. With the average CO/CO_2 ratio of 22 ppb ppm^{-1} for anthropogenic emissions from above, the net biogenic source of CO could be mistaken for an anthropogenic CO_2 flux of maximal 0.4 μmol m^{-2} s^{-1}, i.e., 2.5% of the measured NEE. This negligible contribution is confirmed by our experiment with the observed CO flux translating to an anthropogenic CO_2 flux of 0.1 ± 0.5 μmol m^{-2} s^{-1}. Thus for the given experimental conditions CO proved to be a sensitive tracer for the separation of anthropogenic and biogenic CO_2 fluxes, in that the influence of artifacts due to the net biogenic CO flux was negligible.

[56] The major problem with using CO as a tracer of anthropogenic CO_2 emissions in populated Western Europe comes from the uncertainty in the emission ratios for the various source categories. For instance, the CO/CO_2 emission ratio from energy production (flue gas) is about a factor 1000 smaller than that from automobile exhaust [*Fontelle et al.*, 2000] (see http://citepa.org), which exhibits large variations for different motor concepts, catalytic converter efficiency and driving conditions. Consequently, the average CO/CO_2 emission ratio depends on the relative contribution of different sources, on their regional distribution and seasonal variations and the degree of mixing within the atmosphere. In order to solve this dilemma, reliable detailed emission inventories of both CO and CO_2 are needed.

[57] Another possibility would be to use more than only one tracer of fossil fuel combustion. In case of nitrogen oxides (NO_x), for example, the emission ratio from energy production (flue gas) is only about a factor 2 smaller than that from automobile exhaust [*Fontelle et al.*, 2000]. In our experiment, the mixing ratio of NO_x was almost constant with differences between the stacks of less than 0.1 ppb. Therefore the measured regional CO_2 flux can be unambiguously attributed to the regional daytime NEE.

4.3. Potential and Limitations of the Lagrangian Approach

[58] The advantage of the Lagrangian approach is evidently the removal of the advection term, which exhibits major uncertainty in the traditional (Eulerian) CBL approach, from the budget equation. The chosen flight pattern, consisting of stacks of horizontal legs at several altitude levels in the BL, allows the determination of a mean BL value that is representative of the average mixing ratio transported by advection, independently of turbulent eddies and small scale heterogeneity. In comparison, it was shown that mean BL values determined from a few vertical profiles as in previous CBL approaches are associated with relatively large representativeness errors even under the rather homogeneous "ideal" conditions of our experiment. This problem would be even more important in regions with more heterogeneous land cover.

[59] The uncertainty of the Lagrangian experiment can be reduced in future experiments by improving the quality of the in situ CO_2 measurements which, in principle, can reach an accuracy of 0.1–0.2 ppm [*Daube et al.*, 2002; *Filippi et al.*, 2003]. The methodical uncertainty is partly due to the specific meteorological conditions where a cloud layer prevented direct measurements in the FT. This problem could be overcome by an aircraft with capability for instrumental operation to traverse cloud layers. It is clear, however, that using more than one aircraft enhances substantially the representativeness, and would also allow the upper boundary condition and the upstream CO_2 profile to be monitored. The remaining error is eventually dominated by the uncertainty of w_+, which is difficult to measure and thus has to be obtained from theory and modeling.

[60] The major difficulty with a Lagrangian experiment is the need for fulfilling true Lagrangian conditions, which proved successful only for one flight out of four during this campaign. This problem is even more important under variable background conditions, in heterogeneous source regions and for larger experimental areas. Besides the use of more than one aircraft this difficulty may be moderated by employing mesoscale or Lagrangian particle models for the flight planning and analysis [e.g., *Lin et al.*, 2003].

[61] Also additional experimental tools such as real-time wind calculation on board the aircraft (now realized), or constant level balloons as tracers can help to meet a truly Lagrangian flight pattern under nonstationary conditions.

5. Conclusions

[62] The experiment presented in this paper demonstrates the great potential of the Lagrangian budgeting approach for accurately estimating CO_2 fluxes at regional scales. While the area Les Landes with its homogeneous and very productive forest and flat terrain and the Atlantic coast upwind certainly provided rather favorable conditions, in particular for the experiment on 23 June, the results lend great hopes to the extension of the methodology to other regions with inhomogeneous land use.

[63] The good agreement between the CO_2 budgets derived with a Lagrangian 1-D model and the CBL approach demonstrates that the CBL method can be applied even when significant vertical tracer gradients exist, i.e., for conditions where the vertical eddy diffusion coefficient is larger than 40 m^2 s^{-1}, provided that the measurements allow an accurate estimate of the average CO_2 concentration in the BL.

[64] We demonstrated the ability of the Lagrangian method to separate regional anthropogenic CO_2 emissions from biogenic activity with the help of CO as a tracer, with a small uncertainty due to biogenic CO production and instrumental artifacts corresponding to detection limit for anthropogenic CO_2 emissions as low as 0.5 μmol m^{-2} s^{-1}. However, the available anthropogenic emission inventories are somewhat uncertain, so we recommend ongoing work on the experimental ''calibration'' of CO/CO_2 emission ratios as well in rural regions as in highly populated areas. The parallel measurement of nitrogen dioxides may support this work by delivering valuable additional information about different combustion sources and their spatial distribution.

[65] We expect the Lagrangian budgeting method to be more generally applied in inhomogeneous and biologically less productive regions. Quite tight constraints of regional daytime NEE should be feasible, given (1) high-precision CO_2 measurements, (2) the capability for instrumental operation of the aircraft to traverse cloud layers, (3) confirmed Lagrangian flight patterns, based on additional experimental equipment and model support, and (4) the use of CO as tracer for anthropogenic CO_2. The major principle limitation of the method concerns temporal coverage. Only daytime inferences of NEE are possible. In fact, in this campaign only one day out of four days provided suitable meteorological conditions for conducting a Lagrangian experiment, which once more highlights the difficulty of a systematic determination of regional NEE from atmospheric measurements only.

[66] The regional carbon balance and its temporal variations cannot be quantified and monitored by one method alone. A major future effort will thus be to develop and control useful integration schemes for the different approaches like, e.g., local eddy correlations data and remotely sensed information, including the use of high-resolution 3-D transport models to simulate and understand the atmospheric CO_2 gradients and variability induced by regional sources and sinks. On the basis of the experience gained in the Airborne CO_2/CO Observations to Access the Regional Carbon Balance (COCA) campaign, the wider area of Les Landes has been selected to execute an intensive regional budgeting experiment in the CarboEurope program. The Lagrangian CBL budgeting method, providing direct observations of regional NEE with quantifiable errors, offers a very valuable tool for the calibration and validation of such integration schemes and represents thus an important step forward to constrain regional CO_2 fluxes.

Appendix A: Estimation of Regional NEE Through Combination of Remote Sensing and Flux Tower Data

[67] The computation of the regional Net Ecosystem Exchange (NEE) for the flight area and the time of the experiment comprises two steps. First, daily values of the gross primary production (GPP, in units of gC m^{-2} d^{-1}) are calculated with a radiation use efficiency model using remote sensing information from MODIS aboard the EOS-Terra satellite. In a second step, the daily values of GPP are converted to noontime NEE with information from the local flux measurements at Le Bray. The necessary steps are as follows:

[68] The model for calculating daily average GPP (equation (A1)) is identical with that used for estimating global carbon fixation [*Running et al.*, 2000]:

$$\mathrm{GPP} = \varepsilon \cdot f\mathrm{APAR} \cdot \mathrm{PAR}. \tag{A1}$$

PAR is the photosynthetically active radiation flux (MJ m^{-2} d^{-1}), fAPAR is the fraction absorbed by the vegetation, and ε is the conversion efficiency of energy to fixed carbon (gC MJ^{-1}) according to equation (A2):

$$\varepsilon = \varepsilon_{\max} \cdot f_1(T_{\min}) \cdot f_2(\mathrm{VPD}), \tag{A2}$$

where $\varepsilon_{\max}$ is the plant specific maximum conversion efficiency derived from the same look-up table of biome properties (BPLUT) as used in the standard global model. The functions f_1 and f_2 describe the influence of meteorological conditions on ε with $T_{\min}$ being the daily minimum air temperature and VPD the daytime average vapor pressure deficit.

[69] The necessary fields of meteorological data (PAR, $T_{\min}$, VPD) are taken from NASA's data assimilation office (DAO-GEOS 4 data) in the same way as for the calculation of the global MODIS GPP/NPP product (MOD17, see http://modis.gsfc.nasa.gov/data/atbd/land_atbd.html). The coefficients fAPAR are estimated from reflectances derived via an inverted radiative transfer model [*Myneni et al.*, 1997] from the MODIS data stream (MOD15A2, version 004; see http://modis.gsfc.nasa.gov/data/atbd/land_atbd.html). Daily values of fAPAR are obtained by linear interpolation between the original values, that represent the most reliable observation during an eight day period (http://modis.gsfc.nasa.gov/data/atbd/land_atbd.html). Periods of cloudiness and times when the sensor is not working properly (indicated by a quality flag) are also filled by interpolation. The interpolation should not introduce significant errors since vegetation structure, particularly in evergreen forests, does not change much over periods of days to weeks.

[70] The resulting spatial field of daily GPP for 23 June 2001 is shown in Figure A1. GPP represents only the carbon uptake of the ecosystem, whereas the net ecosystem exchange represents the difference between respiration (R) and photosynthesis:

$$\mathrm{NEE} = R - \mathrm{GPP}. \tag{A3}$$

In order to establish a relation between daily values of GPP and the corresponding values of NEE during the time over which the experiment took place, the eddy covariance data (half hourly means) for NEE from Le Bray were partitioned into GPP and R. The respiration term R was derived from the covariance fluxes measured at night under turbulent conditions and was then related to soil temperature (T_{soil}) via equation (A4) following the approach of *Lloyd and Taylor* [1994]:

$$R(T_{\mathrm{soil}}) = R(T_{\mathrm{ref}}) \cdot \exp\left[E_0 \cdot \left(\frac{1}{T_{\mathrm{ref}} - T_0} - \frac{1}{T_{\mathrm{soil}} - T_0}\right)\right], \tag{A4}$$

with T_{ref} = 10°C and T_0 = −46.02°C [*Lloyd and Taylor*, 1994], i.e., the threshold temperature below which respiration ceases. The sensitivity E_0 and $R(T_{ref})$ were estimated from the nighttime flux data via nonlinear regression for 14 day and 1 day periods, respectively.

[71] The thus separated covariance fluxes were then used to calculate daily averages of GPP. This calculation was performed for 49 days between May and September that had similar meteorological conditions as the 23 June 2001 regarding ecophysiology, i.e., average daylight VPD <8 hPa, mean air temperature between 15°C and 25°C, and daily integrated global radiation flux >18 MJ m^{-2} (The conditions at the tower site on this day were: daylight VPD 3.3 hPa; mean air temperature 20.2°C; daily global radiation 18.4 MJ m^{-2}). Equation (A5) gives the linear regression between the thus derived daily GPP and the average NEE in the flight time interval (1230–1430 UT), obtained directly from the covariance data:

$$\langle \mathrm{NEE} \rangle_{(1230-1430)} = (-2.05 \pm 0.12)\,\mathrm{GPP}_{\mathrm{daily}} + (3.4 \pm 1.1). \quad \text{(A5)}$$

The correlation coefficient was r^2 = 0.62 and higher-order terms were found not to be significant. The value for NEE given in Table 5 and Figure 6 was then derived by applying equation (A5) to the model derived GPP in Figure A1, and averaging over the flight domain.

[72] In order to estimate the uncertainty of the resulting values for NEE, we must consider the error of the remote sensing driven model estimate of daily GPP and, in addition, the error introduced by the conversion of daily GPP values into values of NEE for the time of the flight. The uncertainty in daily GPP depends on the errors in the meteorological variables and the remote sensing data and the intrinsic uncertainty of the model, none of which can be estimated from first principles. We hence try to estimate the potential error of the modeled daily GPP by comparison with the eddy covariance data at the tower for daily GPP (= daily R − daily NEE), using the same method as above for determination of R. Over the year 2001, the average difference (i.e., the bias) between model estimate and tower data is 0.4 μmol m^{-2} s^{-1} with a standard deviation of ±1.9 μmol m^{-2} s^{-1}. The uncertainty of the conversion from GPP to NEE (equation (A2)) is ±1.4 μmol m^{-2} s^{-1}. Simple error propagation yields a total uncertainty of the model derived NEE for the time of the flight of ±2.4 μmol m^{-2} s^{-1}. This error estimate is slightly too large since the random errors of the covariance data appear in both uncertainties. On the other hand, the conversion from GPP to NEE implicitly assumes that the ecophysiological conditions at the tower and in the flight domain are similar. Deviations from this assumption add to the uncertainty, since potential changes in ecophysiological parameters (e.g., the ratio between leaf nitrogen content and soil organic carbon content) would lead to corresponding changes in the relation between GPP and R and thus in the parameters of the linear regression equation (A5). While this effect causes significant problems in the conversion from GPP to NEE for areas with inhomogeneous land cover, the uncertainty is expected to be less than 30% for the homogeneous Landes forest. Therefore the overall error of the model derived NEE should not be larger than the value of ±3 μmol m^{-2} s^{-1} given in Table 4.

[73] **Acknowledgments.** The research of S.S. was supported by a Marie Curie Fellowship of the EC program "Human Potential" under contract HPMF-CT-2000-00794. The authors are grateful to Claire Valant and Laurence Pépin, who conducted the analysis of the flask samples at LSCE, and to Paul Berbigier, who provided the flux data at the Bray tower. Ingeborg Levin is kindly acknowledged for the analysis of the flask samples at IUP and for stimulating discussions regarding the quality of the in situ CO_2 measurements. We would like to thank Steve Running and his NTSG group members for rapid access to the updated MODIS data stream. Special thanks are due to the pilot Willi Fuchs and the instrumental observer Martin Bäumle. Their skills made a large contribution to the success of the campaign. Additional funding provided by WTP-FZJ for the campaign is kindly acknowledged.

References

Bakwin, P. S., P. P. Tans, D. F. Hurst, and C. Zhao (1998), Measurements of carbon dioxide on very tall towers: Results of the NOAA/CMDL program, *Tellus, Ser. B*, *50*, 401–415.

Baldocchi, D., R. Valentini, S. Running, W. Oechel, and R. Dahlman (1996), Strategies for measuring and modeling carbon dioxide and water vapor fluxes over terrestrial ecosystems, *Global Change Biol.*, *2*, 159–169.

Berbigier, P., J.-M. Bonnefond, and P. Mellmann (2001), CO_2 and water vapour fluxes for 2 years above Euroflux forest site, *Agric. For. Meteorol.*, *108*, 183–197.

Betts, A. K., R. L. Desjardins, and J. I. MacPherson (1992), Budget analysis of the boundary layer grid flights during FIFE 1987, *J. Geophys. Res.*, *97*(D17), 18,533–18,546.

Biraud, S., P. Ciais, M. Ramonet, P. Simmonds, V. Kazan, P. Monfray, S. O'Doherty, T. G. Spain, and S. J. Jennings (2000), European greenhouse gas emissions estimated from continuous atmospheric measurements and radon 222 at Mace Head, Ireland, *J. Geophys. Res.*, *105*(D1), 1351–1366.

Crawford, T. L., R. J. Dobosy, R. T. McMillen, C. A. Vogel, and B. B. Hicks (1996), Air-surface exchange measurement in heterogeneous regions: Extending tower observations with spatial structure observed from small aircraft, *Global Change Biol.*, *2*, 275–285.

Daube, B. C., K. A. Boering, A. E. Andrews, and S. C. Wofsy (2002), A high-precision fast-reponse airborne CO_2 analyzer for in situ sampling from the surface to the middle stratosphere, *J. Atmos. Oceanic Technol.*, *19*, 1532–1543.

Denmead, O. T., M. R. Raupach, F. X. Dunin, H. A. Cleugh, and R. Leuning (1996), Boundary layer budgets for regional estimates of scalar fluxes, *Global Change Biol.*, *2*, 255–264.

Desjardins, R. L., E. J. Brach, P. Alvo, and P. H. Schuepp (1982), Aircraft monitoring of surface carbon dioxide exchange, *Science*, *216*, 733–735.

Desjardins, R. L., et al. (1997), Scaling up flux measurements for the boreal forest using aircraft-tower combinations, *J. Geophys. Res.*, *102*(D24), 29,125–29,133.

Filippi, D., M. Ramonet, P. Ciais, D. Picard, J. C. Le Roulley, M. Schmidt, and P. Nedelec (2003), Greenhouse airborne measurements over Europe, paper presented at the XXVIII General Assembly, Eur. Geophys. Soc., Nice, France.

Fontelle, J.-P., J.-P. Chang, N. Allemand, N. Audoux, S. Beguier, and C. Clement (2000), Inventaire des emission de gaz a effet de serre au cours de la periode 1990–1999, *Rep. 430*, Cent. Interprof. Technique d'Etudes de la Pollution Atmos., Paris.

Gerbig, C., S. Schmitgen, D. Kley, A. Volz-Thomas, K. Dewey, and D. Haaks (1999), An improved fast-response vacuum-UV resonance fluorescence CO instrument, *J. Geophys. Res.*, *104*(D1), 1699–1704.

Gerbig, C., J. C. Lin, S. C. Wofsy, B. C. Daube, A. E. Andrews, B. B. Stephens, P. S. Bakwin, and C. A. Grainger (2003), Toward constraining regional-scale fluxes of CO_2 with atmospheric observations over a continent: 2. Analysis of COBRA data using a receptor-oriented framework, *J. Geophys. Res.*, *108*(D24), 4757, doi:10.1029/2003JD003770.

Gioli, B., et al. (2004), Comparison between tower and aircraft-based eddy covariance fluxes in five regions of Europe, *Agric. For. Meteorol.*, in press.

Gros, V., B. Bonsang, and R. Sarda Esteve (1999), Atmospheric carbon monoxide in situ monitoring by automatic gas chromatography, *Chemosphere*, *1*, 153–161.

Gros, V., K. Tsigaridis, B. Bonsang, M. Kanakidou, and C. Pio (2002), Factors controlling the diurnal variation of CO above a forested area in southeast Europe, *Atmos. Environ.*, *36*, 3127–3135.

Intergovernmental Panel on Climate Change (IPCC) (2001), *Climate Change 2001: The Scientific Basis: Contributions of Working Group I*

to the Third Assessment Report of the Intergovernmental Panel on Climate Change, Cambridge Univ. Press, New York.

Laubach, J., and H. Fritsch (2002), Convective boundary layer budgets derived from aircraft data, *Agric. For. Meteorol.*, *111*, 237–263.

Levin, I., et al. (2002), Three years of trace gas observations over the EuroSiberian domain derived from aircraft sampling—A concerted action, *Tellus, Ser. B*, *54*, 696–712.

Levin, I., et al (2003), Eurosiberian carbonflux-CO_2 intercomparison, in *Report on the Eleventh WMO/IAEA Meeting of Experts on Carbon Dioxide Concentration and Related Tracer Measurement Techniques*, edited by S. Toru and S. Kazuto, pp. 37–54, World Meteorol. Organ. Global Atmos. Watch, Tokyo.

Levy, P. G., A. Grelle, A. Lindroth, M. Mölder, P. G. Jarvis, B. Kruijt, and J. B. Moncrieff (1999), Regional-scale CO_2 fluxes over central Sweden by a boundary layer budget method, *Agric. For. Meteorol.*, *98–99*, 169–180.

Lin, J., C. Gerbig, S. C. Wofsy, A. E. Andrews, B. C. Daube, K. J. Davis, and C. A. Grainger (2003), A near-field tool for simulating the upstream influence of atmospheric observations: The Stochastic Time-Inverted Lagrangian Transport (STILT) model, *J. Geophys. Res.*, *108*(D16), 4493, doi:10.1029/2002JD003161.

Lloyd, J., and J. A. Taylor (1994), On the temperature dependence of soil respiration, *Funct. Ecol.*, *8*, 315–323.

Lloyd, J., et al. (1996), Vegetation effects on the isotopic composition of atmospheric CO_2 at local and regional scales: Theoretical aspects and a comparison between rain forest in Amazonia and a boreal forest in Siberia, *Aust. J. Plant Physiol.*, *23*, 371–399.

Lloyd, J., et al. (2001), Vertical profiles, boundary layer budgets, and regional flux estimates for CO_2 and its $^{13}C/^{12}C$ ratio and for water vapor above a forest/bog mosaic in central Siberia, *Global Biogeochem. Cycles*, *15*, 267–284.

Meijer, H. A. J., H. M. Smid, E. Perez, and M. G. Kreizer (1996), Isotopic characterization of anthropogenic CO_2 emissions using isotopes and radiocarbon analysis, *Phys. Chem. Earth*, *21*(5–6), 483–487.

Myneni, R. B., R. R. Nemani, and S. W. Running (1997), Estimation of global leaf area index and absorbed PAR using radiative transfer model, *IEEE Trans. Geosci. Remote Sens.*, *35*, 1380–1393.

Neininger, B., W. Fuchs, M. Baeumle, A. Volz-Thomas, A. S. H. Prévôt, and J. Dommen (2001), A small aircraft for more than just ozone: MetAir's 'Dimona' after ten years of evolving development, paper presented at the 11th Symposium on Meteorological Observations and Instrumentation, Am. Meteorol. Soc., Albuquerque, N. M.

Pépin, L., M. Schmidt, M. Ramonet, D. E. J. Worthy, and P. Ciais (2001), A new gas chromatographic experiment to analyze greenhouse gases in flask samples and in ambient air in the region of Saclay, report, Inst. Pierre Simon Laplace Notes des Activ. Instrum., Paris.

Potosnak, M. J., S. C. Wofsy, A. S. Denning, T. J. Conway, J. W. Munger, and D. H. Barnes (1999), Influence of biotic exchange and combustion sources on atmospheric CO_2 concentrations in New England from observations at a forest flux tower, *J. Geophys. Res.*, *104*(D8), 9561–9569.

Raupach, M. R., O. T. Denmead, and F. X. Dunin (1992), Challenges in linking atmospheric CO_2 concentrations to fluxes at local and regional scales, *Aust. J. Bot.*, *40*, 697–716.

Ritter, J. A., J. D. W. Barrick, C. E. Watson, G. W. Sachse, G. L. Gregory, B. E. Anderson, M. A. Woerner, and J. E. Collins Jr. (1994), Airborne boundary layer flux measurements of trace species over Canadian boreal forest and northern wetland region, *J. Geophys. Res.*, *99*(D1), 1671–1686.

Running, S. W., P. E. Thornton, R. R. Nemani, and J. Glassy (2000), Global terrestrial gross and net primary productivity from the Earth Observing System, in *Methods in Ecosystem Science*, edited by O. E. Sala et al., pp. 44–57, Springer-Verlag, New York.

Schmidt, M., R. Graul, H. Sartorius, and I. Levin (1996), Carbon dioxide and methane in continental Europe: A climatology, and 222Radon-based emission estimates, *Tellus, Ser. B*, *48*, 457–473.

Stohl, A., and N. E. Koffi (1998), Evaluation of trajectories calculated from ECMWF data against constant volume balloon flights during ETEX, *Atmos. Environ.*, *32*, 4151–4156.

Stull, R. B. (1985), A fair-weather cumulus cloud classification scheme for mixed layer studies, *J. Clim. Appl. Meteorol.*, *24*, 49–56.

Stull, R. B. (1988), *An Introduction to Boundary Layer Meteorology*, Kluwer Acad., Norwell, Mass.

Valentini, R., et al. (2000), Respiration as the main determinant of carbon balance in European forests, *Nature*, *404*, 861–865.

Volz, A., and D. Kley (1985), A resonance fluorescence instrument for the in-situ measurement of atmospheric carbon monoxide, *J. Atmos. Chem.*, *2*, 345–357.

Wofsy, S. C., M. L. Goulden, J. M. Munger, S. M. Fan, and P. S. Bakwin (1993), Net exchange of CO_2 in a mid-latitude forest, *Science*, *260*, 1314–1317.

Y. Brunet, Institut National de la Recherche Agronomique–Bioclimatologie, BP 81, F-33883 Villenave d'Ornon, France. (yves.brunet@bordeaux.inra.fr)

P. Ciais, Laboratoire des Sciences du Climat et de l'Environnement, UMR Commissariat à l'Energie Atomique/Centre National de la Recherche Scientifique 1572, Bat 709, CE L'Orme des Merisiers, F-91191 Gif-sur-Yvette, France. (ciais@lsce.saclay.cea.fr)

H. Geiß, D. Kley, and A. Volz-Thomas, Institut für Chemie und Dynamik der Geosphäre II, Forschungszentrum Jülich, P.O. Box 1913, D-52425 Jülich, Germany. (h.geiss@fz-juelich.de; d.kley@fz-juelich.de; a.volz-thomas@fz-juelich.de)

B. Neininger, MetAir AG, Sonnenberg 27, Hausen am Albis, CH-6313 Menzingen, Switzerland. (neininger@metair.ch)

M. Reichstein, Department of Forest Resources and Environment, University of Tuscia, Via S. Camillo de Lellis, I-01100 Viterbo, Italy. (reichstein@unitus.it)

S. Schmitgen, Chambon, F-87920 Condat-sur-Vienne, France. (s.schmitgen@tiscali.fr)